Tribol Lett (2011) 44:279–285
DOI 10.1007/s11249-011-9846-y

ORIGINAL PAPER

Dry Sliding Contact Between Rough Surfaces at the Atomistic Scale

Peter Spijker · Guillaume Anciaux · Jean-François Molinari

Received: 27 April 2011 / Accepted: 13 August 2011 / Published online: 1 September 2011

Abstract Although, a lot is known about the factors contributing to friction, a complete physical understanding of the origins of friction is still lacking. At the macroscale several laws have long since described the relation between load (Amontons, Coulomb), apparent and real area of contact (Bowden and Tabor), and frictional forces. But it is not yet completely understood if these laws of friction extend all the way down to the atomistic level. Some current research suggests that a linear dependence of friction on the real contact area is observed at the atomistic level, but only for specific cases (indentors and rigid substrates). Because continuum models are not applicable at the atomic scale, other modeling techniques (such as molecular dynamics simulations) are necessary to elucidate the physics of friction at the small scale. We use molecular dynamics simulations to model the friction of two rough deformable surfaces, while changing the surface roughness, the sliding speed, and the applied normal load. We find that friction increases with roughness. Also all sliding cases show considerable surface flattening, reducing the friction close to zero after repetitive sliding. This questions the current view of (static) roughness at the atomistic scale, and possibly indicates that the macroscopic laws of friction break down several orders of magnitude before reaching the atomic scale.

Keywords Nanotribology · Molecular simulation · Surface roughness

P. Spijker (✉) · G. Anciaux · J.-F. Molinari
Computational Solid Mechanics Laboratory, Ecole Polytechnique Fédérale de Lausanne, EPFL, LSMS, IIC-ENAC, IMX-STI, Station 18, 1015 Lausanne, Switzerland
e-mail: peter.spijker@epfl.ch

1 Introduction

At the macroscopic level it is long understood that the force of friction is directly proportional to the applied load and that the apparent contact area does not influence the frictional force [1]. The direct proportionality between the load F_N and the frictional force F yields a dimensionless constant μ known as the friction coefficient $\mu = F/F_N$. The friction coefficient can be determined through experiments—and is used as a model parameter in many mechanical engineering problems. However, it is still not completely understood what the physical mechanisms behind the friction coefficient are. Moreover, the friction coefficient is more a system than merely a material parameter, because it depends on both types of interacting materials.

Because of the unlikely perfect matching of any two real surfaces, the real contact area of two materials is much smaller than the apparent contact area, since the materials only touch at a few high spots of both respective surface landscapes. Therefore, the influence of surface roughness on friction is an important topic in current tribology research [2]. Based on the Hertz theory of elastic contacts [3], Bowden and Tabor [1] found a contradicting non-linear dependence of friction on load, which was resolved assuming the contact interface is not flat but involves many asperities with the number of contacts increasing with load [4]. Greenwood and Williamson [5] improved this theory by assuming Gaussian and exponential height distributions for the asperities. Some drawbacks of the Greenwood–Williamson approach are that it relies on a known height distribution, and that it does not take into account the elastic coupling between asperities. In order to cope with different length scales of asperities at once, Persson proposed a theory based on the auto-correlation of the surface

heights, giving a surface roughness which can be approximated by self-affine fractals [6].

Most of the approaches mentioned above to uncover contact clusters and the origins of friction describe the surface from a continuum mechanics point of view. In the limit of smaller length scales contact occurs finally at the atomistic level, where the continuum theory becomes inadequate [7, 8]. Thus, other types of computational methods are required to investigate the processes at the smallest scale. An example of such a method is molecular dynamics (MD), a particle simulation method. At its core this technique solves Newton's equations of motion for each individual atom in the system under consideration. The interactions between the individual atoms are determined by a potential energy function.

In the past few years, a lot of progress has been made in our understanding of frictional mechanisms at the atomistic level by using MD simulations. The system that attracted most attention is the sliding of a small tip over relatively flat surfaces, in an attempt to model the AFM experimental observations [8–19]. A second system studied involves the normal loading of rough surfaces, either with deformable flat and rigid rough surfaces [20, 21], with one of the surfaces being rigid and flat [22, 23], or two flat surfaces [24, 25]. More recently, we studied a similar system but with two fully deformable and rough surfaces instead [26]. Until now no results for sliding of rough deformable surfaces are reported, although very recent study on two colliding surfaces (both being rough and deformable) has been presented [27]. From the macroscopic viewpoint of friction it is this sliding of rough surfaces that is probably one of the most interesting cases to be investigated, because real surfaces are rough and deformable, and are subject to wear and plastic deformation.

2 Model Set-Up

Here, we present MD simulations of sliding between two rough deformable bodies, where the material is modeled through a Lennard-Jones (LJ) potential [28]

$$V_{\mathrm{LJ}}(r) = 4\epsilon\left[\left(\frac{\sigma}{r}\right)^{12} - \left(\frac{\sigma}{r}\right)^{6}\right], \tag{1}$$

where r is the distance between two atoms, σ their characteristic length, and ϵ the energy at which the potential is at its minimum. By using the LJ potential the material in our model has a face centered cubic (FCC) crystal structure. Examples of such materials are gold, platinum, and aluminum.

We have chosen to use LJ parameters which resemble the bulk strength of aluminum. Based on the density of aluminum (2.70 g/cm^3) and its mass (26.98 g/mol) a crystal lattice constant can be determined (0.404 nm). The simulations should start from a crystal in a stable configuration, and, for this purpose the configuration of minimal energy is used to determine the characteristic length σ. Taking into account, all nearest neighbors up to the fourth layer in the crystal, this equals $\sigma = 0.2596$ nm for aluminum. Using the minimum energy configuration to compute σ ensures that the crystal does not contract or expand in the bulk regions. Based on the mass, density, and Young's modulus of aluminum (68 GPa) we determine the LJ energy parameter using the Cauchy–Born rule at 0 K to be $\epsilon = 10.3014$ kJ/mol. The cut-off radius for the LJ potential is set at 0.6039 nm (which follows also from the minimum energy configuration and at this point the potential is almost zero) and for searching the nearest neighbor list an extra shell with a width of 0.234 nm is added. To avoid discontinuities in the Van der Waals energy the potential is shifted to make sure that at the cut-off radius the potential energy equals zero.

Because real surfaces are unlikely completely clean (for instance due to oxidation, condensation, or material dissimilarity between the two surfaces) we have incorporated this effect by changing the LJ potential between the upper and lower body. The energy parameter is reduced to 10% of its original value, which removes almost all the adhesion between the two bodies.

Whether the LJ potential is suitable for metallic systems like ours can be debated. For metallic systems, it is more common to use a potential given by the Embedded Atoms Method (EAM) [29], although, the use of the LJ potential is not uncommon. Typically, the LJ potential gives rise to more brittle behavior than the EAM potential [30]. Also, the bulk plastic behavior (and thus dislocations) is influenced by the choice of the potential. However, we believe that in our systems bulk plastic effects are of less importance, and together with the strongly reduced adhesive behavior, this does not require the use of a computationally more complex potential. This can be justified by our interest in the general behavior of these systems, rather than in the results for one specific metal. It is noteworthy that the same approach was followed by others as well [13, 15, 21, 23].

One of the major drawbacks of MD is that its computational cost increases rapidly with the number of particles. As we wish to study different types of rough surfaces, loading conditions and sliding velocities, we choose a relatively small periodic system size to keep the computational cost acceptable. The FCC structures we create, measure approximately 13 x 13 nm in the lateral direction. To avoid commensurateness the underlying crystal structure of one body is rotated. The rough surfaces for both FCC crystal bodies were generated using a modified version of the random midpoint displacement algorithm [26, 31], ensuring

that surface is periodic across its boundaries. The Hurst exponent (which determines the self-affine fractal scaling, and thus, also the roughness) is set at 0.8.

In Fig. 1, a schematic depiction of the system set-up is shown. Each of the two bodies (with its rough surface) is shown as well as the subdivision into different regions. For the lower body the bottom region (number 6) is kept fixed at all time, giving the system its support. On the contrary, the highest region of the upper body (number 5) is kept rigid, but is allowed to move as one entity upon an externally applied pressure or externally applied displacement (to maintain a constant sliding velocity and a constant pressure). The two main regions (numbers 1 and 2) are completely free (thus deformable), whereas two small thermostat regions (numbers 3 and 4) are used to control the temperature in the system to be around a few Kelvin, through the use of a Langevin thermostat with the damping constant 250 fs^{-1}. We chose the temperature to be close to 0 K to rule out the effect of thermal crystal oscillations on friction. The size in z-direction of regions 5 and 6 (in terms of number of lattice layers) is 4, for regions 3 and 4 this size is 8, and the main regions 1 and 2 are approximately 40 layers each. It is important to note that although six regions are present in the system, each atom in any region is modeled with the same LJ parameters (except for the interaction between atoms of region 1 and 2). The benefit for naming the regions differently is to simplify both the simulations and the analysis. The integration time step for all simulations is set at 5 fs, periodic boundary conditions are applied only in the lateral directions, and the total time covered in one simulation is 10 ns. A typical system for a MD simulation contains about 217,000 atoms and one production run takes about 60 h on eight processors of a Linux commodity cluster.

In order to investigate the effect of surface roughness, sliding speed, and loading pressure, we have investigated three surface roughnesses (0.2, 0.5, and 1.0 nm RMS roughness), five different normal pressures (uniformly distributed on the interval 0.05–0.25 GPa), and two sliding velocities (2 and 10 m/s). Furthermore, for every situation three different random rough surfaces have been generated, which gives some statistical basis for our results. Typical simulations are carried out to cover 10 ns of real time. The pressure range we have used here is just above the yield strength of aluminum (20 MPa), and causes plastic deformation in the material. Our somewhat high pressures are however not unrealistic, as we model only a small part of a macroscopic contact [6].

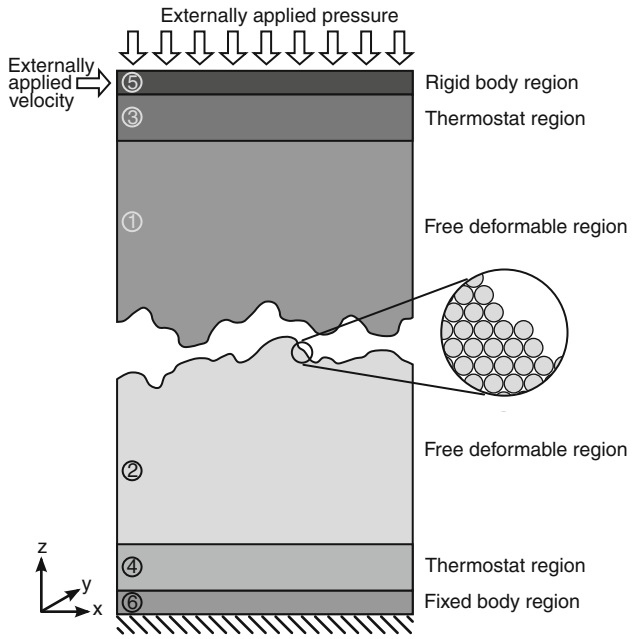

Fig. 1 Schematic representation of the system set-up. The *gray scales* and *numbers* indicate different regions. The *inset* shows that the system has an atomistic representation. The sliding is imposed on the top-most domain only (indicated by the *arrow*) and only in the x-direction. For the lower body the lowest region (*6*) is kept fixed at all time, giving the system its support. More details can be found in the text

3 Results

From the forces between the regions in any of the MD simulations we can determine the friction coefficient, where we used the force in z-direction between regions 3 and 5 as the normal force and the force in x-direction between regions 1 and 2 as the frictional force. In Fig. 2, examples of such instantaneous friction coefficients are

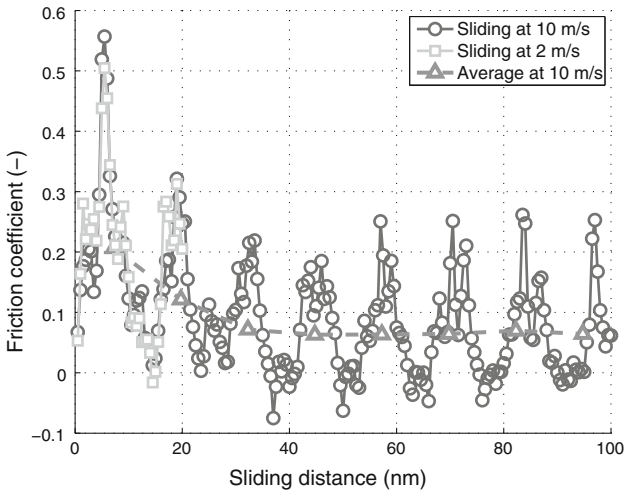

Fig. 2 For the same rough surface (RMS 0.5 nm, load 0.20 GPa) the instantaneous friction coefficient is shown for two different sliding velocities (2 and 10 m/s) as a function of the sliding distance. The *dotted line* gives the average friction coefficient for the 10 m/s case

shown as a function of the sliding distance. It is important to notice that this instantaneous friction coefficient varies considerably over time, but that on average we measure larger and more realistic friction coefficients than reported previously for systems that focus mainly on the sliding of flat surfaces either with LJ or EAM potentials [32, 33]. This indicates that the presence of roughness is important for friction.

Due to the applied sliding velocity and the relatively small periodic system, the upper body moves repeatedly over the lower body (1.5 times for the low speed, and more than 7 times for the high speed, see Fig. 2). It is interesting to note that for our system parameters it does not matter what the sliding speed is (either 2 or 10 m/s); the frictional behavior is similar.

Overall, Fig. 2 reveals that the average friction coefficient is a decreasing function of the sliding distance. Eventually, this decrease leads to friction coefficients much closer to zero, regardless of applied load and initial roughness. However, the general observation of all our simulations is that this average friction coefficient is increasing with increasing roughness, see Fig. 3. We have also observed a minor dependence on applied load (see encircled area in Fig. 3), with lower loads leading to initially higher friction coefficients. This is caused by the fact that with a higher initial load the contacting parts before the sliding starts are already flattened mildly (a few percent RMS roughness change), which, in the absence of adhesion, lowers the initial friction. As such this indicates that there is a large dependence of the friction on the actual topography of the surface.

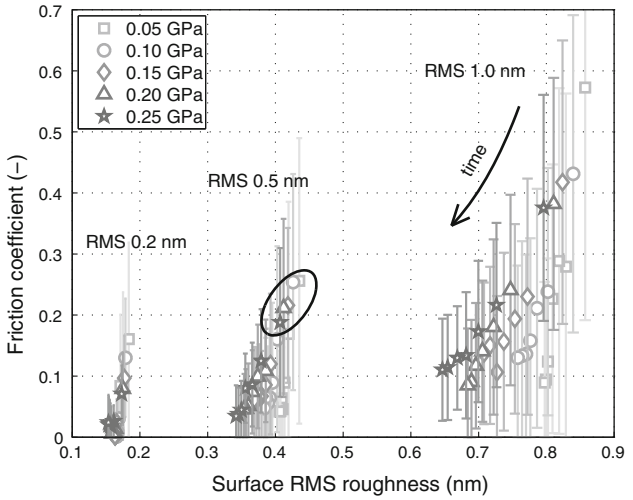

Fig. 3 Dependence of the friction coefficient on the surface roughness for sliding at 10 m/s. *Different markers* indicate different normal loads (see legend in top left corner). Each *marker* indicates the average (and standard deviation) of the friction coefficient for the time it takes to slide the sample once. The "time" *arrow* indicates the direction in which the friction and roughness reduction takes place. The *encircled area* shows five initial friction coefficients, indicating the small dependence of the friction coefficient on applied load

By far the most striking result for all simulations (regardless of initial surface roughness or applied normal pressure) is that during sliding the surfaces become flat rapidly. This flattening can be verified by visual inspection of the simulations (see for example Fig. 4a), but also numerically by computing the RMS roughness and skewness (asymmetry), Fig. 4b, c. These values are computed by superposing a rectangular grid on the surface and translating the atomic positions onto the grid, from which surface statistics can then be collected. The initial surface roughness (Fig. 4b) decreases for all systems, although, the amount of decrease depends on the applied loading (less decrease for lower loads). A similar effect can be seen for the skewness of the height distribution, see Fig. 4c. Initially, the skewness is close to zero, because the surfaces are generated from a Gaussian distribution which has zero skewness, but as the sliding takes place the surfaces become rapidly askew. The tops of the asperities become eventually flat, but it takes longer to do so for the rougher surfaces.

In order to quantify how much of the surfaces become flat and how this relates to the measured friction coefficient, we computed the local slope gradient using the same rectangular grid as for other surface statistics. We consider a part of the surface being flat when the local slope gradient is smaller than 0.25 change of the grid size. Using this criterion, we compute the ratio of the surface being flat with respect to the total surface area. In Fig. 5a, this flatness is related to the friction coefficient for all the systems sliding at 10 m/s, which shows an exponential decrease for the friction coefficient with increasing flatness (indicated by the dashed line being a least square fit of an equation of the type $a\ \mathrm{e}^{-bx}$).

We pointed out before that the initial topography of the surface is important with respect to the friction. This also can be concluded from the large deviations we observe in the friction coefficient if we use different rough surfaces, see Fig. 3, although even these deviations vanish when the sliding distance increases. As such our data supports the ideas proposed by Fineberg [34] in his recent discussion that atomic scale roughness is important when determining frictional resistance as well as observations from earlier 2D MD simulations [23].

What we observed is that the asperities are flattened rather easily, but that their debris does not necessarily fill all the valleys of the rough surfaces, otherwise the surfaces would no longer be askew. The tops of asperities are more or less smeared out in the direction of the sliding, which enlarges the lateral size of the asperities and meanwhile lowers them, see Fig. 5b.

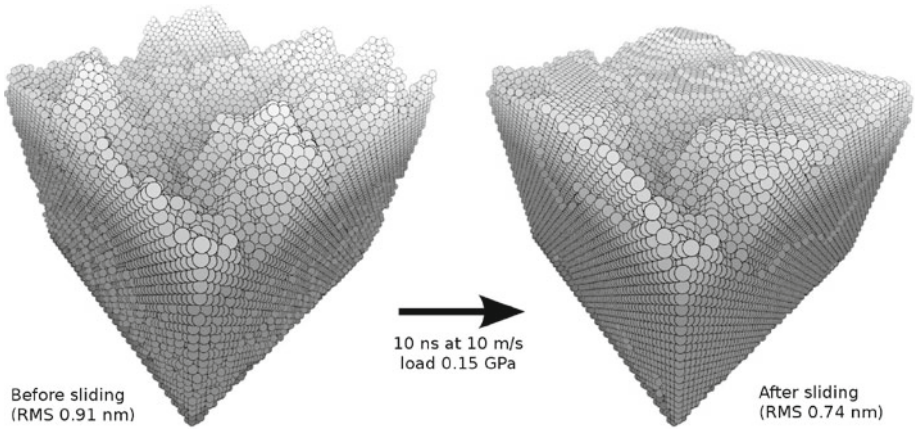

(a) Surface flattening

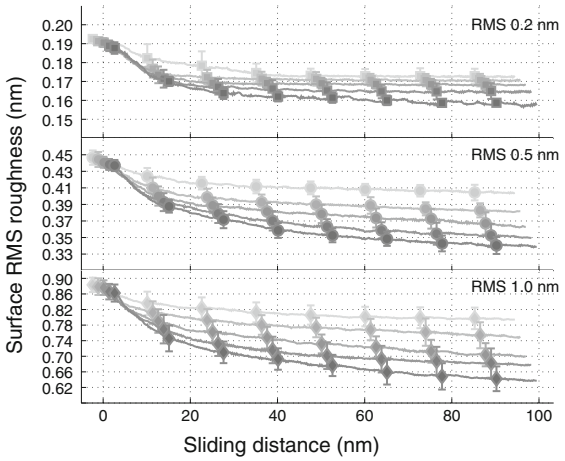

(b) Surface RMS roughness

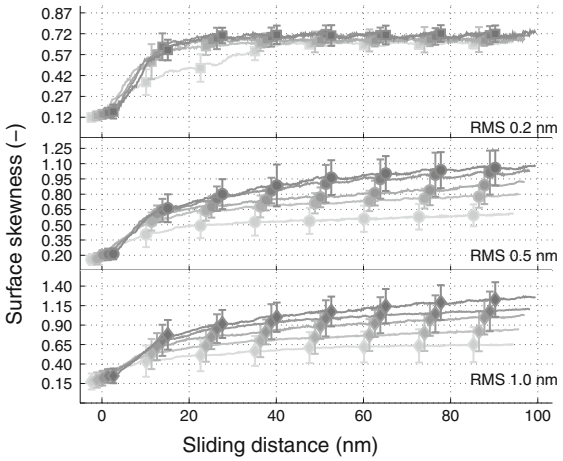

(c) Surface skewness

Fig. 4 Effect of sliding at 10 m/s: **a** illustrating the amount of flattening during sliding the bottom surface of the same system, **b** decrease of the RMS roughness, and **c** increase of the skewness of the height distribution. In each of the two figures different RMS roughnesses are from top to bottom and for every applied pressure (*gray* shades indicate applied normal pressure, *dark* means a higher pressure) as a function of sliding distance

4 Conclusion and Discussion

The final structures of all rough surfaces in our simulations are very similar. The valleys of the surfaces remain almost unchanged, whereas the original asperities all have a flat surface. In the end, the friction is dominated by the sliding of two flat surfaces (albeit with holes in the surface). It has already been reported before that it is not uncommon for flat surfaces to exhibit no friction at all [24, 25], and, thus it is to be expected that we see the measured friction to go to zero as well. Moreover, we see an inverse relationship between the amount of surface flattening and the measured friction coefficient.

The view on friction of rough surfaces at the atomistic scale we propose, given the system under consideration, is the following. Atomistic scale asperities are not very stable in the case of (repetitive) sliding and loading and are flattened easily. This flattening does not lead to completely flat surfaces, but rather to flat surfaces with holes in it, where the holes are still the original valleys of the rough surface. The system is in equilibrium when the holes of both sides are arranged in such a way that the surfaces are always sufficiently in contact somewhere to support the load. It is thus the sum of both surface profiles (see Fig. 5c) that determines whether the system is in equilibrium (with too many or too large holes the contacting surfaces cannot support the load and will be flattened further until they can). Finally, the sliding that occurs is only flat on flat and this reduces, in the absence of adhesion, the friction to almost zero. However, it is also observed that the systems with initial higher roughness do not reach the same flatness as the systems with lower roughness (see Fig. 5a). This could indicate that some of these surfaces are not yet entirely flattened or that the presence of larger asperities

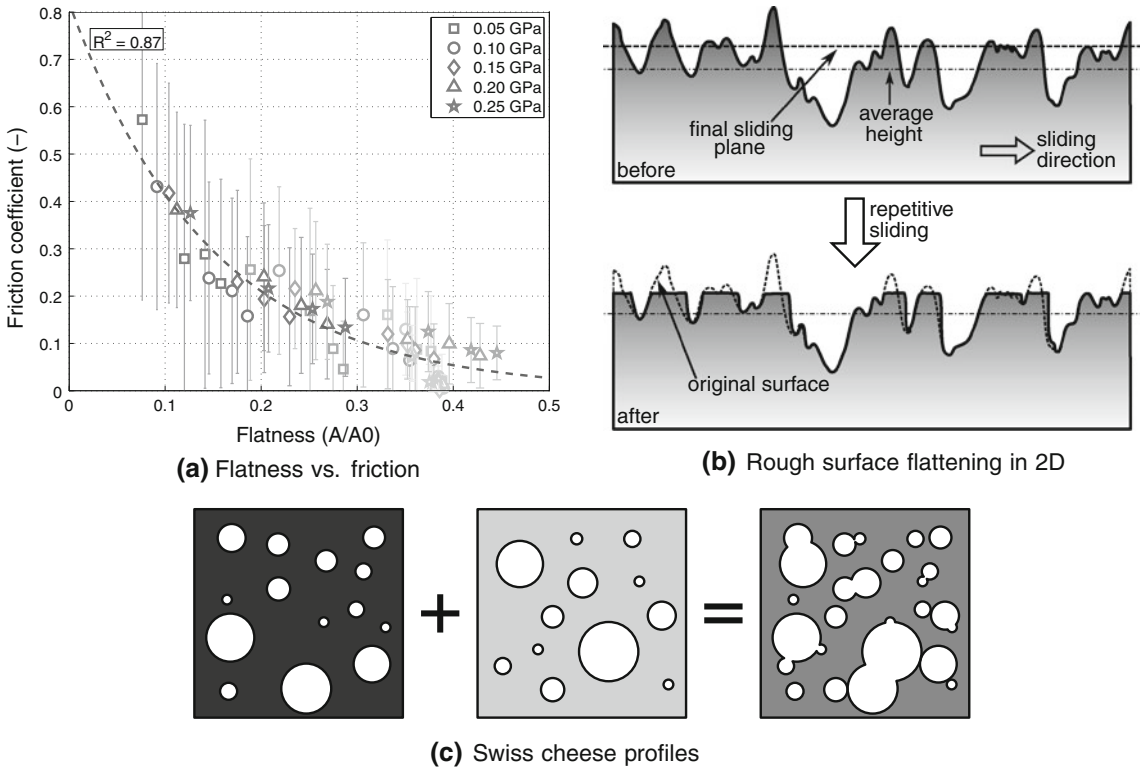

Fig. 5 In **a**, the relation between flatness (see text for an explanation) and the friction coefficient is shown (for all results at 10 m/s), including an exponential least square fit (*dashed line*, with a regression coefficient of 0.87). The *symbols* indicate different pressures and the *gray shades* different initial RMS roughness, *dark* means a higher initial roughness. In **b**, a schematic representation of the flattening of a rough surface (depicted in 2D) is shown. The original surface is flattened at the final sliding plane (which is above the average height), and the material is displaced in the sliding direction. The valleys are not filled from the bottom but become a little less wide instead. In **c**, it is depicted that the flattening of rough surfaces is not total, as holes are left on the surface. The holes are the original valleys of the rough surface, and the size and amount of them depends on the initial surface roughness and loading pressure. The system is in equilibrium when the holes of both sides are arranged in such a way that the surfaces are always sufficiently in contact somewhere in order to support the load

(due to the initial higher roughness), even if they are flattened, still remain as obstacles for the sliding and as such dictate the amount of friction, preventing it from reaching zero.

The observations on the sliding of two rough surfaces described in this study can partially be influenced by the choice of interaction potential in the MD simulations. Here, we have chosen to reduce the adhesive properties of the LJ considerably, but to investigate the effect of this, we also performed some of the simulations without this reduced adhesion for the system with a 0.5 nm RMS roughness. This showed a much higher roughness reduction (from 0.50 to 0.20 nm, compared to 0.35 nm) and after 10 ns of sliding the surfaces are almost completely flat, but due to the stronger adhesion the apparent friction coefficient remained much higher ($\mu_{\text{adh}} = 1.5$ and $\mu_{\text{non-adh}} = 0.1$), indicating that in this case the adhesive properties dominate the friction more than the surface roughness does. Currently, we are investigating in more depth the effects of adhesion on the frictional properties using a similar system set-up.

Instead of a LJ potential, the EAM potential is often preferred in metallic systems. In order to qualitatively investigate the potential dependence, we randomly choose one of our systems (RMS roughness 0.5 nm, 0.15 GPa load, and sliding speed 10 m/s) and changed the bulk potential from LJ to EAM. We measured very similar friction coefficients (both around 0.05) and surface roughness changes as with the full LJ system, which increases our confidence in all of our results with the LJ system. The major difference observed by visual inspection showed a part of the upper surface being ripped off and being integrated into the lower surface (due to our implemented contact algorithm, see [26]). Very quickly after this major event the remaining sliding surfaces became flat as well and we reached a similar steady state as with the LJ system.

In the case of stronger adhesion or in the presence of third bodies or a lubricant it can be expected that the flattening of the surface is stopped and that these other processes increase the likelihood of roughness being

recreated, because these third bodies can scratch the surface. Therefore, in real systems this asperity flattening could well be less prominent, although this is not yet confirmed. Preliminary results for simulations where small rigid nanoparticles (2 nm diameter) are added as lubricant, show that the RMS roughness is reduced less but also that the friction is very close to zero, because the rigid nanoparticles act as roller bearings.

In this study, we have shown that friction in the presence of limited adhesion is an increasing function of roughness. The surface topography plays a crucial role in the actual amount of friction. Moreover, due to repetitive sliding the rough surfaces become flat rapidly and consequently the friction approached zero. The type of surfaces we observe finally resemble a Swiss cheese: flat with holes.

Acknowledgments The research described in this article is supported by the European Research Council (ERCstg UFO-240332) and the Swiss National Science Foundation (Grant No. 200021_122046/1).

References

1. Bowden, F.P., Tabor, D.: The Friction and Lubrication of Solids. Oxford University Press, Oxford, United Kingdom (2001)
2. Blau, P.J.: The significance and use of the friction coefficient. Tribol. Int. **34**, 585–591 (2001)
3. Johnson, K.L.: Contact Mechanics. Cambridge University Press, Cambridge (1985)
4. Archard, J.F.: Contact and rubbing of flat surfaces. J. Appl. Phys. **24**, 981–988 (1953)
5. Greenwood, J.A., Williamson, J.B.P.: Contact of nominally flat surfaces. Proc. R. Soc. Lond. A **295**, 300–319 (1966)
6. Persson, B.N.J., Albohr, O., Tartaglino, U., Volokitin, A.I., Tosatti, E.: On the nature of surface roughness with application to contact mechanics, sealing, rubber friction and adhesion. J. Phys. Condens. Matter **17**, R1–R62 (2005)
7. Luan, B., Robbins, M.O.: The breakdown of continuum models for mechanical contacts. Nature **435**, 929–932 (2005)
8. Luan, B., Robbins, M.O.: Contact of single asperities with varying adhesion: comparing continuum mechanics to atomistic simulations. Phys. Rev. E **74**, 026111 (2006)
9. Sørensen, M.R., Jacobsen, K.W., Stoltze, P.: Simulations of atomic-scale sliding friction. Phys. Rev. B **53**, 2101–2113 (1996)
10. Buldum, A., Ciraci, S., Batra, I.P.: Contact, nanoindentation, and sliding friction. Phys. Rev. B **57**, 2468–2476 (1998)
11. Knippenberg, M.T., Mikulski, P.T., Dunlap, B.I., Harrison, J.A.: Atomic contributions to friction and load for tip-self-assembled monolayers interactions. Phys. Rev. B **78**, 235409 (2008)
12. Mo, Y., Turner, K.T., Szlufarska, I.: Friction laws at the nanoscale. Nature. **457**, 1116–1119 (2009)
13. Cheng, S., Luan, B., Robbins, M.O.: Contact and friction of nanoasperities: effects of adsorbed monolayers. Phys. Rev. E **81**, 016102 (2010)
14. Crill, J.W., Ji, X., Irving, D.L., Brenner, D.W., Padgett, C.W.: Atomic and multi-scale modeling of non-equilibrium dynamics at metalmetal contacts. Model. Simul. Mater. Sci. Eng. **3**, 034001 (2010)
15. Kim, W.K., Falk, M.L.: Accelerated molecular dynamics simulation of low-velocity frictional sliding. Model. Simul. Mater. Sci. Eng. **3**, 034003 (2010)
16. Knippenberg, M.T., Mikulski, P.T., Harrison, J.A.: Effects of tip geometry on interfacial contact forces. Model. Simul. Mater. Sci. Eng. **3**, 034002 (2010)
17. Perez, D., Dong, Y., Martini, A., Voter, A.F.: Rate theory description of atomic stick-slip friction. Phys. Rev. B **81**, 245415 (2010)
18. Li, Q., Dong, Y., Perez, D., Martini, A., Carpick, R.W.: Speed dependence of atomic stick-slip friction in optimally matched experiments and molecular dynamics simulations. Phys. Rev. Lett. **106**, 126101 (2011)
19. Dong, Y., Perez, D., Voter, A.F., Martini, A.: The roles of statics and dynamics in determining transitions between atomic friction regimes. Tribol. Lett. **42**, 99–107 (2011)
20. Yang, C., Persson, B.N.J.: Molecular dynamics study of contact mechanics: contact area and interfacial separation from small to full contact. Phys. Rev. Lett. **100**, 024303 (2008)
21. Yang, C., Persson, B.N.J.: Contact mechanics: contact area and interfacial separation from small contact to full contact. J. Phys. Condens. Matter **20**, 215214 (2008)
22. Campañà, C., Müser, M.H., Robbins, M.O.: Elastic contact between self-affine surfaces: comparison of numerical stress and contact correlation functions with analytic predictions. J. Phys. Condens. Matter **20**, 354013 (2008)
23. Luan, B., Robbins, M.O.: Hybrid atomistic/continuum study of contact and friction between rough solids. Tribol. Lett. **36**, 1–16 (2009)
24. Dienwiebel, M., Verhoeven, G.S., Pradeep, N., Frenken, J.W.M., Heimberg, J.A., Zandbergen, H.W.: Superlubricity of graphite. Phys. Rev. Lett. **92**, 126101 (2004)
25. Pastewka, L., Moser, S., Gumbsch, P., Moseler, M.: Anisotropic mechanical amorphization drives wear in diamond. Nat. Mater. **10**, 34–38 (2010)
26. Spijker, P., Anciaux, G., Molinari, J.F.: The effect of loading on surface roughness at the atomistic level, Comput. Mech. Published online (2011). doi:10.1007/s00466-011-0574-9
27. Delogu, F.: Molecular dynamics of collisions between rough surfaces. Phys. Rev. B **82**, 205415 (2010)
28. Lennard-Jones, J.E.: Cohesion. Proc. Phys. Soc. **43**, 461–482 (1931)
29. Daw, M.S., Baskes, M.I.: Embedded-atom method: derivation and application to impurities, surfaces, and other defects in metals. Phys. Rev. B **29**, 6443–6453 (1984)
30. Abraham, F.F., Rudge, W.E., Alexopoulos, P.S.: Fragmentation dynamics in asperity collisions: a molecular dynamics simulation study. Comput. Mater. Sci. **3**, 21–40 (1994)
31. Miller, G.S.P.: The definition and rendering of terrain maps, In: SIGGRAPH '86: Proceedings of the 13th Annual Conference on Computer Graphics and Interactive Techniques, pp. 39–48. ACM, New York, NY (1986)
32. Robbins, M.O., Müser, M.H.: Computer simulations of friction, lubrication and wear. In: Bhushan, B., (ed.) Handbook of Modern Tribology, pp. 717–765. CRC Press, Boca Raton, FL (2000)
33. Mosey, N.J., Müser, M.H.: Atomistic modeling of friction. Rev. Comput. Chem. **25**, 67–124 (2007)
34. Fineberg, J.: Tribology: diamonds are forever—or are they?. Nat. Mater. **10**, 3–4 (2010)